Sub Topic: Internal Combustion and Gas Turbine Engines

11th U.S. National Combustion Meeting
Organized by the Western States Section of the Combustion Institute
March 24–27, 2019
Pasadena, California

Nonlinear dynamics of closely spaced thermoacoustic modes in the presence of noise

Tony John[1,], Ghirardo Giulio[2], Vishal Acharya[1], Mirko Bothien[2], and Timothy Lieuwen[1]*

[1]*School of Aerospace Engineering, Georgia Institute of Technology, 270 Ferst Drive, Atlanta, GA, 30332, USA*
[2]*Ansaldo Energia Switzerland, Baden 5401, CH*
[*]*Corresponding author: tjohn8@gatech.edu*

Abstract: Practical combustion systems can have linearly unstable axial thermoacoustic modes that oscillate at close frequencies. These modes are nonlinearly coupled and their interaction can result in novel dynamics when the frequency spacing is much smaller compared to the mean frequency of oscillations. In this study, we consider frequency spacing of up to 10 percent of the mean frequency. In a recent paper, Acharya et al. (*Combustion and Flame* 2018) showed that a mode with larger growth rate could be suppressed depending on the frequency spacing between the modes. In this paper, we extend the work by Acharya et al. to include the effects of noise in the system and we explore how the deterministic dynamics change in the presence of noise. Noise can alter the behavior of the system significantly by changing the average amplitudes and the stability of the limit cycle oscillations. In order to study these noise-induced features, we derive the stochastic evolution equations for the amplitudes and phases of the two modes using an averaging procedure. Then, we analyze the dynamics of the system in its state space and numerically obtain the probability density functions of amplitudes and phases for a set of parameters. For sufficiently high noise intensity, we observe that both modes coexist and the system switches between them in an irregular manner when they evolve in time.
Keywords: ***Thermoacoustic oscillations, stochastic dynamics***

1. Introduction

Lean premixed combustors are susceptible to large amplitude pressure and velocity oscillations known as thermoacoustic instability. This instability occurs when a positive feedback loop is established between the unsteady heat release rate and the acoustic modes of the combustor [1–3]. As a result of this coupling, the pressure and velocity fluctuations can grow in amplitude and eventually saturate to a large amplitude oscillatory state. These oscillations can reduce the performance of the combustor and in the worst case lead to increased wear [4, 5]. Therefore, it is important to predict the onset of thermoacoustic oscillations and the amplitude of the oscillations attained by the system.

A linear analysis could be adopted to predict the transition to thermoacoustic oscillations. However, this analysis cannot determine the amplitude and frequency of the limit cycle oscillations or detect any complex dynamical features displayed by the system. In order to completely describe these dynamical states, it is important to understand the nonlinear features of the system. For gas

turbine combustors, the nonlinearity mainly arises from the response of the flame to acoustic perturbations. This nonlinear response can be approximately quantified using the Flame Describing Function [6]. A Flame Describing Function provides the response of the flame to a sinusoidal input at the forcing frequency. The response at all other frequencies other than the forcing frequency are neglected in this formulation. This approach works well when the system has a single dominant frequency. In many practical combustors, there could be two modes that are linearly unstable and their natural frequencies could be different from each other. In such cases, a Flame Double Input Describing Function can be adopted to quantify the nonlinearity in heat release rate response [7, 8]. This is an extension to the Flame Describing Function framework where the flame is now forced with two amplitudes and two frequencies. Orchini and Juniper [9] has shown that this approach is useful in accurately predicting the stability, frequency and amplitude of quasi-periodic oscillations. In this paper, we analyze a system of two coupled thermoacoustic modes that are closely spaced in the frequency domain. In general, a Flame Double Input Describing Function formulation need to be used when the system has two distinct frequencies. However, we can still adopt a single describing function approach if the frequency spacing between the modes is small. The details of this approximation are provided in Section 2.

In a recent work, Acharya et al. [10] used the method of averaging and derived evolution equations for a system of closely spaced thermoacoustic modes. The averaging procedure can be adopted for this system since the frequency spacing between the modes is small. Acharya et al. [10] showed that a mode with larger growth rate could be suppressed and the mode with lower growth rate could evolve to a limit cycle. Such non-trivial dynamics occur when the modes are closely spaced and the spatial mode shapes satisfy certain conditions. In this paper, we extend the work by Acharya et al. [10] to include effects of background noise on the dynamics of closely spaced modes. It is important to understand the stochastic characteristics of the system since practical combustion systems operate in a turbulent environment. So, the response of the flame to incoherent background fluctuations need to be taken into account to fully describe the system. These background fluctuations can alter the qualitative features of the system. For instance, it can change the average amplitudes of the limit cycle oscillations or the stability characteristics of the system [11]. These noise sources can also affect the evolution of each mode differently. So, a stochastic analysis might be necessary to explain some of the behavior observed in experiments.

The aim of this work is to develop a framework to analyze the dynamics of closely spaced thermoacoustic modes in the presence of noise. The framework developed here follows the work by Giulio et al. [12] on azimuthal thermoacoustic modes although the equations derived here are for closely spaced modes. Then, we explore how the conclusions derived from a deterministic analysis can change when the system evolves in the presence of noise. Further, we look for any novel dynamical features displayed by the noisy system that cannot be revealed by a deterministic analysis.

2. Mathematical formulation

The governing equations for the coupled thermoacoustic modes are derived from the non-dimensional inhomogeneous wave equation given by [13].

$$\frac{\partial^2 p}{\partial t^2} - \Delta^2 p = (\gamma - 1)\tilde{q}\delta(\mathbf{x} - \mathbf{x}_f) \tag{1}$$

where p is the acoustic pressure and $\tilde{q}$ is the fluctuating heat release rate. We assume that the heat release is concentrated at the burner location ($\mathbf{x}_f$). The acoustic pressure can be expanded using the Galerkin formulation as [3, 13].

$$p(\mathbf{x},t) = \dot{\eta}_1(t)\psi_1(\mathbf{x}) + \dot{\eta}_2(t)\psi_2(\mathbf{x}) \tag{2}$$

The fluctuating heat release rate can be decomposed into

$$\tilde{q} = \tilde{Q} + \tilde{q}_s \tag{3}$$

where $\tilde{Q}$ and $\tilde{q}_s$ are the deterministic and the stochastic part of the unsteady heat release rate respectively. The deterministic function $\tilde{Q} = \tilde{Q}[p_f(t)]$ at the flame location is given as

$$\tilde{Q} = \tilde{Q}[\dot{\eta}_1\psi_1(\mathbf{x}_f) + \dot{\eta}_2\psi_2(\mathbf{x}_f)] \tag{4}$$

where p_f is the pressure fluctuation at the flame location. Define the function $Q = (\gamma - 1)\tilde{Q}$. Substitute (2), (3) and (4) into (1). Then project it along each eigenfunction (ψ_1 and ψ_2) to obtain the following coupled oscillator equations

$$\ddot{\eta}_1 + \omega_1^2\eta_1 = \frac{\psi_1(\mathbf{x}_f)}{\Lambda_1}Q[\dot{\eta}_1\psi_1(\mathbf{x}_f) + \dot{\eta}_2\psi_2(\mathbf{x}_f)] - \frac{\tilde{\alpha}_1}{\Lambda_1}\dot{\eta}_1 + \frac{\tilde{\sigma}_1}{\Lambda_1}\xi(t) \tag{5a}$$

$$\ddot{\eta}_2 + \omega_2^2\eta_2 = \frac{\psi_2(\mathbf{x}_f)}{\Lambda_2}Q[\dot{\eta}_1\psi_1(\mathbf{x}_f) + \dot{\eta}_2\psi_2(\mathbf{x}_f)] - \frac{\tilde{\alpha}_2}{\Lambda_2}\dot{\eta}_2 + \frac{\tilde{\sigma}_2}{\Lambda_2}\xi(t) \tag{5b}$$

where $\xi(t)$ is a noise term obtained from the following integral (for the first mode)

$$\frac{\gamma - 1}{\Lambda_1}\int_\Omega \tilde{q}_s(\mathbf{x},t)\psi_1(\mathbf{x})dV = \frac{\tilde{\sigma}_1}{\Lambda_1}\xi(t) \tag{6}$$

where $\tilde{\sigma}_1$ and Λ_1 are constants. Note that the stochastic part of the unsteady heat release rate $\tilde{q}_s$ is assumed to be acoustically compact in (6). We can derive a similar expression for the noise term in (5b) for the second mode. We assume that $\xi(t)$ is a Gaussian noise source with $\langle\xi(t)\rangle = 0$ and $\langle\xi(t)\xi(t+\tau)\rangle = \delta(\tau)$. Denote $\alpha_1 = \tilde{\alpha}_1/\Lambda_1, \alpha_2 = \tilde{\alpha}_2/\Lambda_2, \sigma_1 = \tilde{\sigma}_1/\Lambda_1$ and $\sigma_2 = \tilde{\sigma}_2/\Lambda_2$.
Introduce change of variables $\dot{\eta}_1 = A_1(t)\cos(\omega_1 t + \varphi_1(t))$ and $\dot{\eta}_2 = A_2(t)\cos(\omega_2 t + \varphi_2(t))$. For simplicity, set $\psi_1(\mathbf{x}_f) = \psi_2(\mathbf{x}_f) = 1$. If we assume that the amplitude and phase functions are slowly varying with respect to the frequency of oscillation, then we can derive the following relations.

$$\eta_1 = \frac{A_1}{\omega_1}\sin(\omega_1 t + \varphi_1) \tag{7a}$$

$$\eta_2 = \frac{A_2}{\omega_2}\sin(\omega_2 t + \varphi_2) \tag{7b}$$

We can also get two constraint equations that link the time derivatives of amplitude and phase given by

$$\dot{A}_1\sin(\omega_1 t + \varphi_1) + A_1\dot{\varphi}_1\cos(\omega_1 t + \varphi_1) = 0 \tag{8a}$$

$$\dot{A}_2 \sin(\omega_2 t + \varphi_2) + A_2 \dot{\varphi}_2 \cos(\omega_2 t + \varphi_2) = 0 \tag{8b}$$

Substitute (7), (8) into (5). Then perform the following change of variables

$$A_1 = A\cos\left(\frac{\pi}{4} + \chi\right) \tag{9a}$$

$$A_2 = A\sin\left(\frac{\pi}{4} + \chi\right) \tag{9b}$$

where $\chi \in [-\pi/4, \pi/4]$. Rewrite (2) to obtain the following expression for pressure fluctuations at the flame location

$$p(\mathbf{x}_f, t) = p_f(t) = \tilde{A}\cos(\bar{\omega}t + \bar{\phi}) \tag{10}$$

where $\bar{\omega} = (\omega_1 + \omega_2)/2$ and $\tilde{A}$ is defined as

$$\tilde{A} = \sqrt{(A_2 - A_1)^2 \sin^2\frac{\theta}{2} + (A_2 + A_1)^2 \cos^2\frac{\theta}{2}} \tag{11}$$

where $\theta = \Delta\omega t + \varphi_2 - \varphi_1$, $\Delta\omega = \omega_2 - \omega_1$ and

$$\bar{\phi} = \bar{\varphi} + \arctan\left(\tan\chi \tan\frac{\theta}{2}\right) \tag{12}$$

Then, we can express $\tilde{A}$ in terms of A, χ and θ as follows (using the definition (11))

$$\tilde{A}^2 = A^2(1 + \cos 2\chi \cos\theta) \tag{13}$$

We introduce these new variables $\tilde{A}$ and $\bar{\phi}$ so that we can express the heat release rate response $Q[p_f(t)]$ using a single describing function. We can see from (10) that the pressure fluctuations at the flame location can be expressed in terms of a single amplitude and phase function. Now, define the flame describing function $S(\tilde{A}, \bar{\omega})$ as

$$S(\tilde{A}, \bar{\omega}) = \frac{1}{\tilde{A}}\frac{\bar{\omega}}{\pi}\int_0^{\frac{2\pi}{\bar{\omega}}} Q[\tilde{A}\cos(\bar{\omega}t)]e^{-\iota\bar{\omega}t}dt \tag{14}$$

Note that $\mathrm{Im}[S(\tilde{A})] = 0$. Perform stochastic averaging [14] to obtain the following equations.

$$\begin{aligned}\dot{A} =& \frac{\tilde{A}^2\,\mathrm{Re}[S(\tilde{A})]}{4A}\left(\frac{1}{\Lambda_1} + \frac{1}{\Lambda_2}\right) + \frac{A\,\mathrm{Re}[S(\tilde{A})]}{4}\sin 2\chi\left(\frac{1}{\Lambda_2} - \frac{1}{\Lambda_1}\right) - \frac{A}{4}(\alpha_1 + \alpha_2) - \frac{A}{4}\sin 2\chi(\alpha_2 - \alpha_1) \\ &+ \frac{\sigma_1^2}{4A} + \frac{\sigma_2^2}{4A} - \frac{\sigma_1\sigma_2\cos 2\chi\cos\theta}{4A} + \frac{\sin 2\chi}{8A}(\sigma_1^2 - \sigma_2^2) - \frac{\sigma_1\sigma_2\cos\theta}{4A}\sec 2\chi + \xi_A\end{aligned} \tag{15a}$$

$$\begin{aligned}\dot{\chi} =& \frac{\mathrm{Re}[S(\tilde{A})]}{4}(\cos 2\chi + \cos\theta)\left(\frac{1}{\Lambda_2} - \frac{1}{\Lambda_2}\right) - \frac{\mathrm{Re}[S(\tilde{A})]}{4}\sin 2\chi\cos\theta\left(\frac{1}{\Lambda_2} + \frac{1}{\Lambda_1}\right) + \frac{(\alpha_1 - \alpha_2)}{4}\cos 2\chi \\ &+ (\sigma_1^2 - \sigma_2^2)\frac{\cos 2\chi}{4A^2} + \frac{\sigma_1\sigma_2\sin 2\chi\cos\theta}{2A^2} + \frac{\sigma_2^2}{8A^2}\left(\frac{1 - \sin 2\chi}{\cos 2\chi}\right) - \frac{\sigma_1^2}{8A^2}\left(\frac{\cos 2\chi}{1 - \sin 2\chi}\right) + \xi_\chi\end{aligned} \tag{15b}$$

$$\dot{\theta} = \Delta\omega - \frac{\mathrm{Re}[S(\tilde{A})]}{2}\sin\theta\Big(\frac{1-\sin 2\chi}{\Lambda_2\cos 2\chi} + \frac{\cos 2\chi}{\Lambda_1(1-\sin 2\chi)}\Big) + \frac{\sigma_1\sigma_2\sin\theta}{2A^2\cos 2\chi} + \xi_\theta \tag{15c}$$

where the noise terms follow $\langle\xi_i\rangle = 0$ and $\langle\xi_i(t)\xi_j(t+\tau)\rangle = 2K_2^{i,j}\delta(\tau)$ and

$$K_2^{A,A} = \frac{\sigma_1^2}{8}(1-\sin 2\chi) + \frac{\sigma_1\sigma_2}{4}\cos\theta\cos 2\chi + \frac{\sigma_2^2}{8}(1+\sin 2\chi) \tag{16a}$$

Similarly, we can get the following relations

$$K_2^{A,\chi} = \frac{\sigma_1^2}{8A}(1-\sin 2\chi) - \frac{\sigma_2^2}{8A}(1+\sin 2\chi) \tag{16b}$$

$$K_2^{A,\theta} = -\frac{\sigma_1\sigma_2}{2}\frac{\sin\theta\sec 2\chi}{A} \tag{16c}$$

$$K_2^{\chi,\chi} = \frac{\sigma_1^2}{8A^2}(1-\sin 2\chi) - \frac{\sigma_1\sigma_2}{4A^2}\cos\theta\cos 2\chi + \frac{\sigma_2^2}{8A^2}(1+\sin 2\chi) \tag{16d}$$

$$K_2^{\chi,\theta} = -\frac{\sigma_1\sigma_2}{4}\frac{\sin\theta}{A^2}\Big(\frac{1-\cos 4\chi - 2\sin 2\chi}{\cos 2\chi(1-\sin 2\chi)}\Big) \tag{16e}$$

$$K_2^{\theta,\theta} = \frac{\sigma_1^2}{2A^2(1-\sin 2\chi)} + \frac{\sigma_2^2}{2A^2(1+\sin 2\chi)} - \frac{\sigma_1\sigma_2}{A^2\cos 2\chi}\cos\theta \tag{16f}$$

Interpreting the variables $A, 2\chi$ and θ as spherical coordinates, it is easy to visualize the phase space of the system. $\theta \in [-\pi, \pi]$ is the longitude angle and $2\chi \in [-\pi/2, \pi/2]$ is the latitude angle. A refers to the amplitude in the radial direction. A similar geometric interpretation of the system in spherical coordinates is presented in Giulio and Bothien [15]. In this coordinate system, if the solution lies near $\chi = \pi/4$, it means that the second mode is dominant. Similarly, if if the solution lies near $\chi = -\pi/4$, then the first mode is the dominant mode. Note that a mode is considered dominant when the amplitude of that mode is larger than the other mode. θ is the synchronization parameter that shows the total phase difference between the two modes.

3. Results

In the following analyses, we consider a describing function of the form

$$\mathrm{Re}[S(\tilde{A})] = \beta - \kappa\tilde{A}^2 \tag{17}$$

where β and κ are constants. A common tool used to study the dynamics of nonlinear deterministic systems is the phase portrait. This portrait reveals the trajectories that are followed by the system for any given initial condition. It helps in detecting any attractors, repellors or any invariant surfaces in the system. For noisy systems, we can obtain similar phase portraits termed as stochastic phase portraits [16]. These portraits are derived from Ito stochastic differential equations by setting the diffusion matrix to zero. This gives rise to a set of ordinary differential equations which can then be analyzed in the phase space. These differential equations include the effect of drift introduced by the noise terms in the system. Note that Eq. (15) is a set of Ito equations. So, we set

the diffusion matrix K_2 to zero and analyze the resulting set of differential equations in the phase space.

The phase portrait of the system (15) in the $\chi - \theta$ plane is shown in Fig. 1(a). The system is mapped on to the surface given by $\dot{A} = 0$ in order to obtain this phase plot. The vector field is given by the blue streamlines in the plot. The green-yellow colormap shows the magnitude of he vector field. The thick and dashed black lines denote the χ and θ nullclines respectively. Since the phase portrait is obtained on the $\dot{A} = 0$ surface, fixed points can be identified as those points where the thick and dashed lines coincide. The streamlines show that θ keeps increasing expect near the fixed points. Since this is a 3D system, we will need to consider an additional surface to get a complete picture of the phase space. So, we consider the phase portrait along a $\theta =$ constant plane as shown in Fig. 1(b). The value of the constant in this figure is 1.8. We can see that all the streamlines converge towards the $\dot{A} = 0$ surface and the long term evolution is constrained to this surface. On this surface, the system moves in the direction of increasing θ i.e., the system revolves around along the latitude lines and approach one of the attractors situated near the poles. Also we can observe a saddle like region on the $\dot{A} = 0$ line that demarcates the basin of attraction of the two attractors.

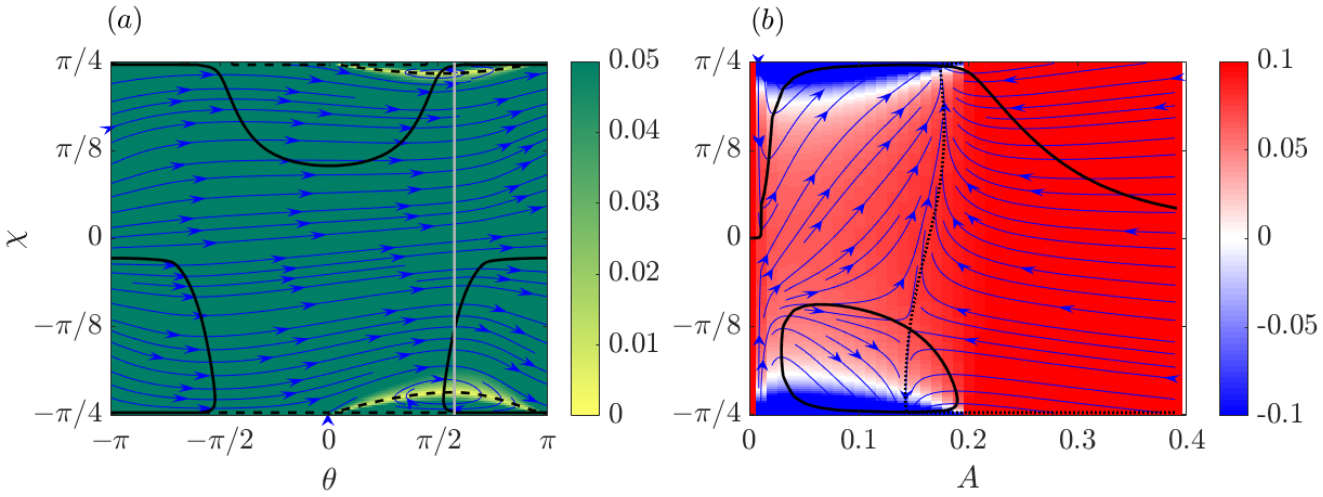

Figure 1: The stochastic phase plot (a) in the $\chi - \theta$ plane obtained along the $\dot{A} = 0$ surface and in the (b) $\chi - A$ surface obtained along $\theta = 1.8$. The grey vertical line in (a) corresponds to $\theta = 1.8$. The green-yellow colormap shows the magnitude of the $\chi - \theta$ vector field. The red-blue colormap shows the value of $\dot{\theta}$. The dotted line is the nullcline, the thick line is the χ nullcline and the dashed line is the θ nullcline. Parameters are $\beta = 0.04, \kappa = 1, \alpha_1 = 0.02, \alpha_2 = 0.01, \bar{\omega} = 1, \Delta\omega = 0.1, \sigma_1 = \sigma_2 = 2 \times 10^{-3}, \Lambda_1 = \Lambda_2 = 1$.

We can also numerically obtain the probability density functions of A, χ and θ for the same set of parameters (see Fig. 2). We see that both modes can be dominant since there are two distinct peaks in the pdf of χ. However, the mode with lower damping coefficient (mode 2 in this case) is the *most probable dominant mode*. We can explain this behavior using the phase portrait in Fig. 1(b). Note that the attractor close to $\chi = \pi/4$ has a larger basin of attraction. This means

that there is a higher chance of visiting this attractor when you run time domain simulations of the stochastic differential equations. Even if we provide initial conditions close to the solution $\chi = -\pi/4$, the system can evolve towards the solution near $\chi = \pi/4$ given enough time. This behavior where the dominant mode "hops" has been observed in experiments [17]. Note that $\Lambda_1 = \Lambda_2$ in this case which corresponds to the situation where the feedback from the heat release rate fluctuations on each mode is the same.

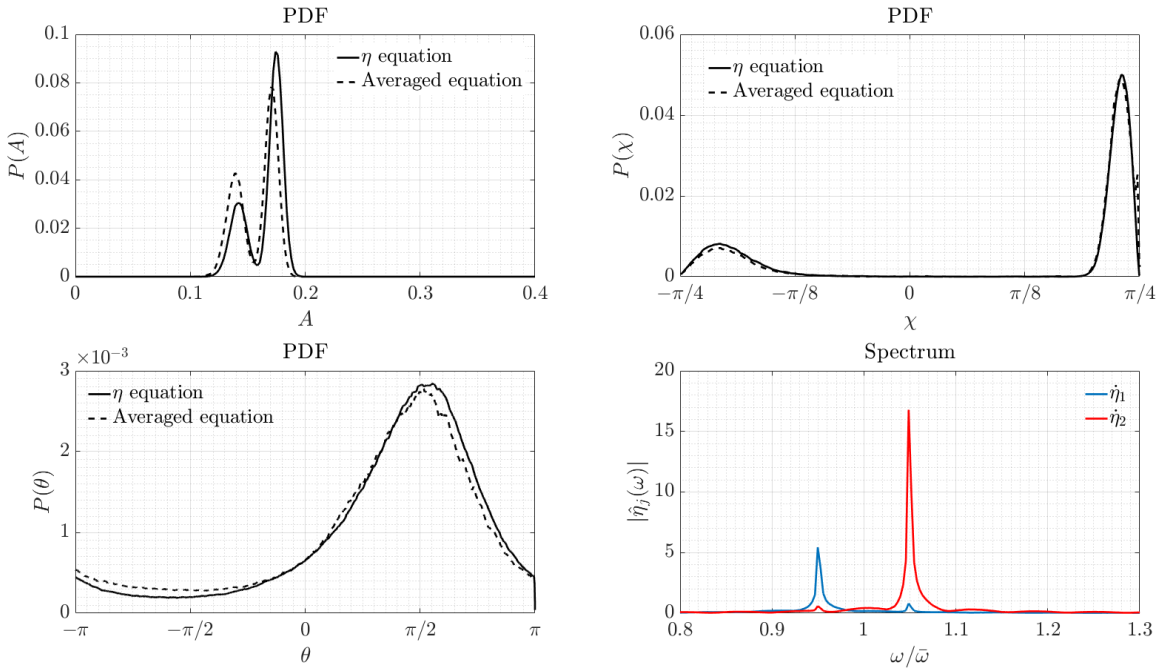

Figure 2: The pdfs of A, χ and θ along with the amplitude specta of η_1 and η_2. Parameters are $\beta = 0.04, \kappa = 1, \alpha_1 = 0.02, \alpha_2 = 0.01, \bar{\omega} = 1, \Delta\omega = 0.1, \sigma_1 = \sigma_2 = 2 \times 10^{-3}, \Lambda_1 = \Lambda_2 = 1$.

In Fig. 3, we present stochastic phase portraits obtained for a higher noise intensity. We can notice that the nullclines do not cross each other in Fig. 3(a). So there are no fixed points visible in the phase portrait. However, we can notice two main regions where the magnitude of the vector field are very small. Since the noise intensity is high in this case, the system can easily switch between these two regions which we call "attractors". This means that the dominant mode keeps switching in an irregular manner as the system evolves in time. From the corresponding pdfs presented in Fig. 4, we can see that the system remains near the attractor close to $\chi = \pi/4$ for a longer period of time. Therefore, the second mode (the mode with lower damping coefficient) is the *most probable dominant mode* although the dominant mode keeps switching in time. Now if we pay our attention to the phase portrait in Fig. 3(b), we can see the point where the A and χ nullclines cross will be observed for any θ section we consider (compare with Fig. 3(a)). Also, this point attracts all the nearby streamlines. So, in the phase space, this will look like a limit cycle oscillation. So a bifurcation in the system has occurred as the noise intensity is increased from 2×10^{-3} to $1 \times 10^{-}2$.

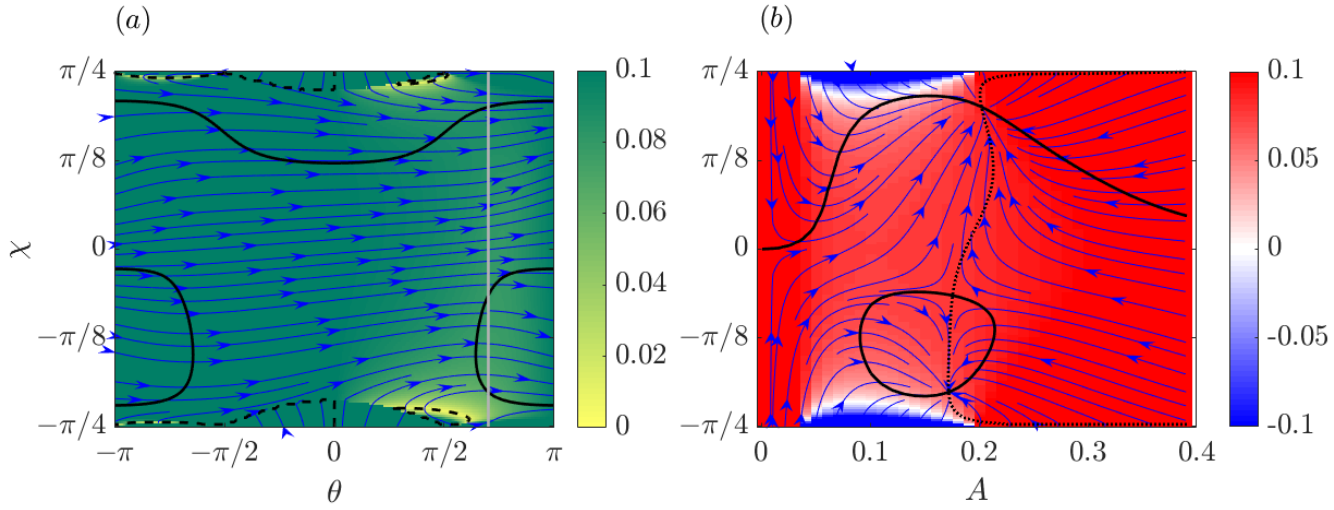

Figure 3: The stochastic phase plot (a) in the $\chi - \theta$ plane obtained along the $\dot{A} = 0$ surface and in the (b) $\chi - A$ surface obtained along $\theta = 2.2$. The grey vertical line in (a) corresponds to $\theta = 2.2$. The green-yellow colormap shows the magnitude of the $\chi - \theta$ vector field. The red-blue colormap shows the value of $\dot{\theta}$. The dotted line is the A nullcline, the thick line is the χ nullcline and the dashed line is the θ nullcline. Parameters are $\beta = 0.04, \kappa = 1, \alpha_1 = 0.02, \alpha_2 = 0.01, \bar{\omega} = 1, \Delta\omega = 0.1, \sigma_1 = \sigma_2 = 1 \times 10^{-2}, \Lambda_1 = \Lambda_2 = 1$.

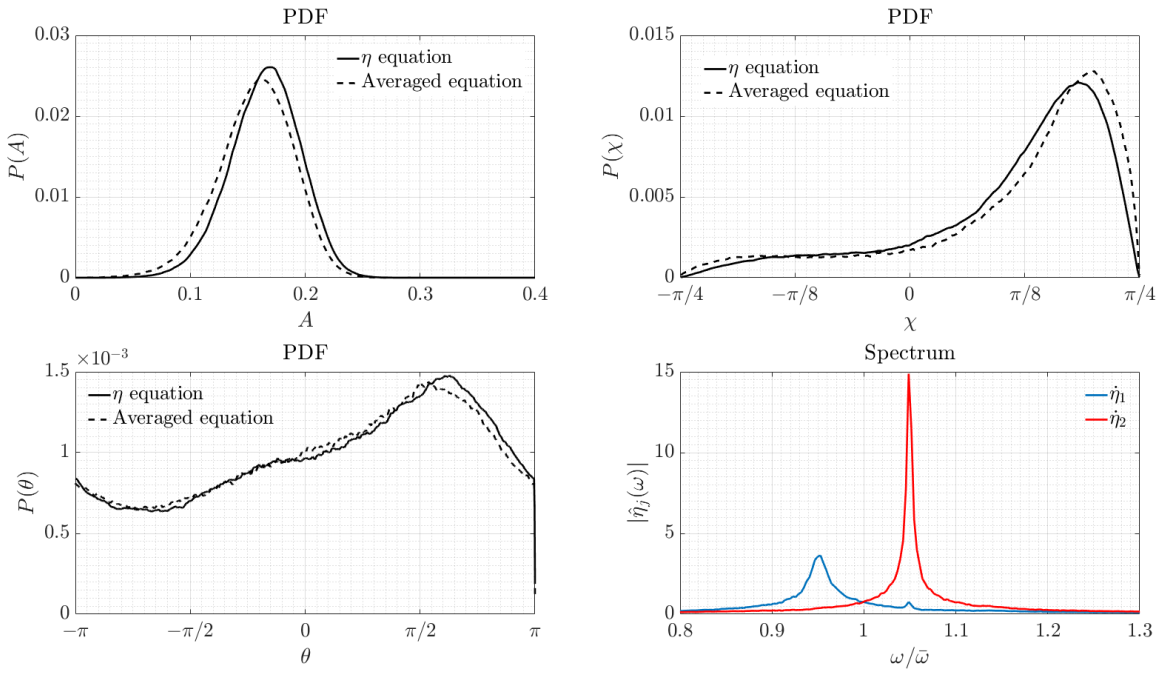

Figure 4: The pdfs of A, χ and θ along with the amplitude specta of $\dot{\eta}_1$ and $\dot{\eta}_2$. Parameters are $\beta = 0.04, \kappa = 1, \alpha_1 = 0.02, \alpha_2 = 0.01, \bar{\omega} = 1, \Delta\omega = 0.1, \sigma_1 = \sigma_2 = 1 \times 10^{-2}, \Lambda_1 = \Lambda_2 = 1$.

4. Conclusions

This paper investigates the dynamics of two closely spaced thermoacoustic modes in the presence of noise. This system is modeled using a set of coupled oscillator equations that are perturbed by noise. In this study, we use a single describing function formulation to approximate the nonlinear feedback of the flame to both modes. Then, we adopt the stochastic averaging procedure to derive the evolution equation for the amplitudes and phase difference of the two modes. We identify a new set of state variables A, χ and θ that enable us to obtain a geometric interpretation of the system.

We analyze this system using stochastic phase portraits and the probability density functions of the variables A, χ and θ obtained numerically. We identify the qualitative features of the system for two sets of noise intensities. For low noise, we find that both modes can be dominant. However, the most probable dominant mode is the one with lower damping coefficient (for the set of parameters considered in this study). For higher noise level, the behavior of the system is qualitatively different. In this case, we find that there are no fixed points in the system. However, a limit cycle-like attractor appears in the phase space. This means that the dynamics of the system is qualitatively different when compared to the low noise case. Further, the dominant mode keeps switching in an irregular manner as the system evolves in time.

5. Acknowledgements

This research was funded by ...

References

[1] F. E. C. Culick, Combustion Instabilities in Liquid-Fueled Propulsion Systems — An Overview, AGARD Conference Proceedings (NATO, Neuilly Sur Seine, France) 450 (1988) 1–73.

[2] K. R. McManus, T. Poinsot, and S. M. Candel, A review of active control of combustion instabilities, Prog. Energy Combust. Sci. 19 (1993) 1–29.

[3] T. C. Lieuwen, Unsteady Combustor Physics, Cambridge University Press, 2012.

[4] A. C. Altunlu, P. J. M. van der Hoogt, and A. de Boer, Sensitivity of Combustion Driven Structural Dynamics and Damage to Thermo-Acoustic Instability: Combustion-Acoustics-Vibration, J. Eng. Gas Turbines Power 136 (2014) 051501.

[5] E. H. Perry and F. E. C. Culick, Measurements of Wall Heat Transfer in the Presence of Large-Amplitude Combustion-Driven Oscillations, Combust. Sci. Technol. 9 (1974) 49.

[6] A. Gelb and W. Vander Velde, Multiple input Describing Functions and Nonlinear System Design, McGraw-Hill Book, 1968.

[7] A. P. Dowling, Nonlinear self-excited oscillations of a ducted flame, J. Fluid Mech. 346 (1997) 271–290.

[8] A. P. Dowling and S. R. Stow, Acoustic Analysis of Gas Turbine Combustors, J. Prop. Power 19 (2003) 751–764.

[9] A. Orchini and M. P. Juniper, Flame Double Input Describing Function analysis, Combust. Flame 171 (2016) 87–102.

[10] V. S. Acharya, M. R. Bothien, and T. C. Lieuwen, Non-linear dynamics of thermoacoustic eigen-mode interactions, Combust. Flame 194 (2018) 309–321.

[11] T. C. Lieuwen, Statistical characteristics of pressure oscillations in a premixed combustor, J. Sound Vib. 260 (2003) 3–17.

[12] G. Giulio, F. Boudy, and M. R. Bothien, Amplitude statistics prediction in thermoacoustics, J. Fluid Mech. 844 (2018) 216–246.

[13] F. E. C. Culick, Nonlinear behavior of acoustic waves in combustion chambers—I, Acta Astronautica 3 (1976) 715–734.

[14] V. S. Anishchenko, V. Astakhov, A. Neiman, T. Vadivasova, and L. S. Geier, Nonlinear Dynamics of Chaotic and Stochastic Systems, Springer Berlin Heidelberg, 2007.

[15] G. Giulio and M. R. Bothien, Quaternion structure of azimuthal instabilities, Phys. Rev. Fluids 3 (2018) 113202.

[16] M. Mendler, J. Falk, and B. Drossel, Analysis of stochastic bifurcations with phase portraits, PLoS ONE 13 (2018) e0196126.

[17] N. Noiray, D. Durox, T. Schuller, and S. Candel, A unified framework for nonlinear combustion instability analysis based on the flame describing function, J. Fluid Mech. 615 (2008) 139–167.